

## SPECTRAL ENERGY DISTRIBUTIONS AND AGE ESTIMATES OF 78 STAR CLUSTERS IN M33

JUN MA,<sup>1</sup> XU ZHOU,<sup>1</sup> JIANGSHENG CHEN,<sup>1</sup> HONG WU,<sup>1</sup> ZHAOJI JIANG,<sup>1</sup> SUIJIAN XUE,<sup>1</sup> AND JIN ZHU<sup>1</sup>

Received 2002 January 29; accepted 2002 February 19

### ABSTRACT

In this third paper of our series, we present CCD spectrophotometry of 78 star clusters that were detected by Chandar, Bianchi, & Ford in the nearby spiral galaxy M33. CCD images of M33 were obtained as a part of the BATC Multicolor Sky Survey of the sky in 13 intermediate-band filters from 3800 to 10000 Å. By aperture photometry, we obtain the spectral energy distributions of these 78 star clusters. As Chandar, Bianchi, & Ford did, we estimate the ages of our sample clusters by comparing the photometry of each object with theoretical stellar population synthesis models for different values of metallicity. We find that the sample clusters formed continuously in M33 from  $\sim 3 \times 10^6$  to  $10^{10}$  yr. This conclusion is consistent with Chandar, Bianchi, & Ford. The results also show that there are two peaks in cluster formation at  $\sim 8 \times 10^6$  and  $\sim 10^9$  yr in these clusters.

*Key words:* galaxies: evolution — galaxies: individual (M33) — galaxies: star clusters

### 1. INTRODUCTION

The importance of the study of star clusters is difficult to overstate, especially in Local Group galaxies. Star clusters, which represent, in distinct and luminous “packets,” single age and single abundance points and encapsulate at least a partial history of the parent galaxy’s evolution, can provide a unique laboratory for studying. For example, globular clusters can be used to provide a lower limit to the age of the parent galaxy, provided their ages can be ascertained, and to study the properties of the parent galaxy soon after its formation.

M33 is a small Scd Local Group galaxy about 15 times farther from us than the LMC (distance modulus is 24.64) (Freedman, Wilson, & Madore 1991; Chandar, Bianchi, & Ford 1999a). It is interesting and important because it represents a morphological type intermediate between the largest “early-type” spirals and the dwarf irregulars in the Local Group (Chandar et al. 1999a). In addition, at a distance of  $\sim 840$  kpc, M33 is the only nearby late-type spiral galaxy; it can provide an important link between the cluster populations of earlier-type spirals (Milky Way and M31) and the numerous, nearby later-type dwarf galaxies. A database of star clusters for M33 have been yielded from the ground-based work (Hiltner 1960; Kron & Mayall 1960; Christian & Schommer 1982, 1988; Melnick & D’Odorico 1978; Mochejska et al. 1998) and from the *Hubble Space Telescope* (*HST*) images (Chandar et al. 1999a; Chandar, Bianchi, & Ford 2001). In specific, the *HST* spatial resolution allowed Chandar et al. (1999a, 2001) to penetrate the crowded, spiral regions of M33, yielding the unbiased, representative sample of star clusters, which can be used to probe the global properties of M33. Since clusters at the distance of M33 are easily distinguished from stellar sources in *HST* WFPC2 images, the clusters detected by *HST* WFPC2 images are reliable.

Using the *HST* WFPC2 multiband images of 20 fields in M33, Chandar et al. (1999a) detected 60 star clusters in this spiral galaxy. These clusters sample a variety of environments from outer regions to spiral arms and central regions

and are the first unbiased, representative sample of star clusters in M33. Then, Chandar, Bianchi, & Ford (1999b) estimated the ages and masses for these star clusters by comparing the integrated photometric measurements with evolutionary models and theoretical  $M/L_V$  ratios. They found the 60 star clusters to form continuously in their parent galaxy from  $\sim 4 \times 10^6$  to  $10^{10}$  yr and to have masses between  $\sim 4 \times 10^2$  and  $3 \times 10^5 M_\odot$ .

M33 was observed as part of galaxy calibration program of the Beijing-Arizona-Taiwan-Connecticut (BATC) Multicolor Sky Survey (Fan et al. 1996; Zheng et al. 1999) from 1995 September 23 to 2000 August 28. This program uses the 60/90 cm Schmidt telescope at the Xinglong Station of Beijing Astronomical Observatory (BAO) and has a custom-designed set of 15 intermediate-band filters to do spectrophotometry for preselected  $1 \text{ deg}^2$  regions of the northern sky. The BAO Schmidt telescope is equipped with a Ford  $2048 \times 2048$  CCD at its main focus. Using the 13 intermediate-band filters images of M33 obtained from the BATC Multicolor Sky Survey, Ma et al. (2001) studied the 60 star clusters of Chandar et al. (1999a). They (Ma et al. 2001) presented the spectral energy distributions (SEDs) by aperture photometry and estimated the ages by comparing the integrated photometric measurements with theoretical stellar population synthesis models for these star clusters. We can provide the accurate SEDs for these star clusters using the multicolor photometry of BATC.

From 35 deep *HST* WFPC2 fields, Chandar et al. (2001) again detected 102 star clusters in M33, 82 of which had not previously been detected. Using one dereddened color  $[(V-I)_0]$ , they estimated the ages and masses for these clusters with single stellar population models. However, they did not give quantitative age estimates for individual clusters because of the relatively large uncertainty associated with age estimates from comparison of one color with single stellar population models.

In this paper, we present the SEDs of 78 star clusters that were detected by Chandar et al. (2001) in M33 and quantitatively estimate the ages for these clusters by comparing the integrated photometric measurements with theoretical stellar population synthesis models.

The outline of the paper is as follows: Details of observations and data reduction are given in § 2. In § 3, we provide a

<sup>1</sup> National Astronomical Observatories, Chinese Academy of Sciences, Beijing, 100012, China; majun@vega.bac.pku.edu.cn.

brief description of the stellar population synthesis models of G. Bruzual & S. Charlot (1996, unpublished). The age estimates for the star clusters are given in § 4. The summary and discussion are presented in § 5.

## 2. SAMPLE OF STAR CLUSTERS, OBSERVATIONS, AND DATA REDUCTION

### 2.1. *Sample of Star Clusters*

The sample of star clusters in this paper is from Chandar et al. (2001), who used 35 deep *HST* WFPC2 fields to extend the search for star clusters in M33 and particularly to focus on detection of older clusters. Since these clusters cover a range of environments from the center to the skirts, they can be used to probe the global properties of the parent galaxy. At the same time, the accurate positions of these star clus-

ters are presented in Chandar et al. (2001). As a result, we select these star clusters to be studied and obtain their SEDs in the 13 intermediate-band filters by aperture photometry. The age estimates for these star clusters are obtained using the theoretical evolutionary population synthesis methods. Clusters 63, 65, 66, 80, 82, 85, 102, 105, 111, 123, 134, 138, 140, 143, and 149 are not included in our sample because of their low signal-to-noise ratio in the images of some BATC filters. In addition, clusters 61, 70, 81, 90, 98, 104, 106, 114, and 116 are U49, M9, C20, U77, R14, H38, H10, C38, and R12 of Christian & Schommer (1982), respectively, the SEDs and ages of which were presented (Ma et al. 2002) and are also not included in our sample. The position of cluster 85 presented by Chandar et al. (2001) may be wrong. It should be R.A. =  $01^{\text{h}}33^{\text{m}}14^{\text{s}}.28$ , decl. =  $30^{\circ}28'22''.9$ , and it is U137 of Christian & Schommer (1982; see details from Ma et al. 2002).

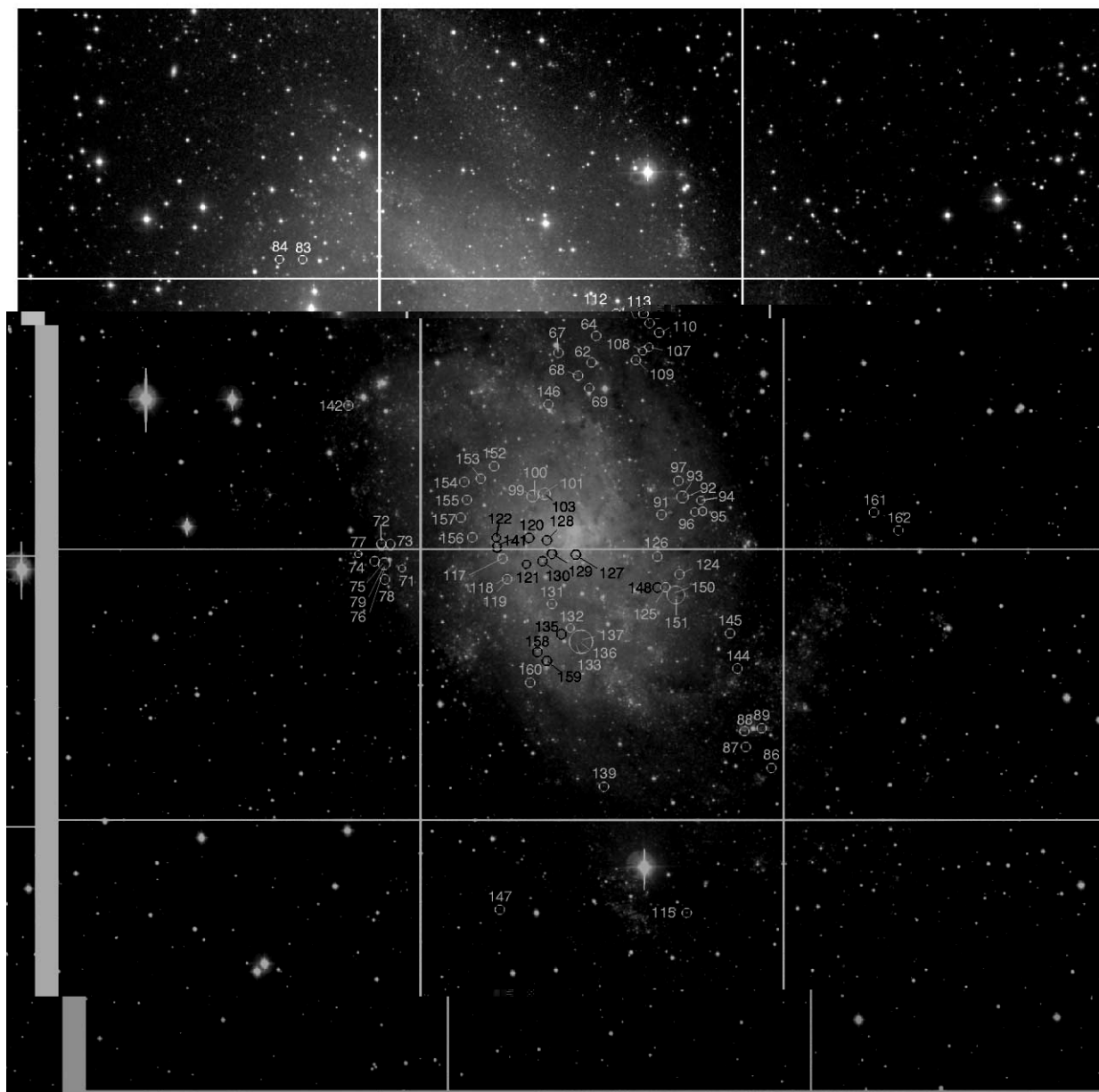


FIG. 1.—Image of M33 in filter BATC07 ( $5785 \text{ \AA}$ ) and the positions of the sample star clusters. The image size is  $52' \times 53'$ . The center of the image is located at R.A. =  $01^{\text{h}}33^{\text{m}}50^{\text{s}}.58$ , decl. =  $30^{\circ}39'08''.4$  (J2000.0). North is up, and east is to the left.

Figure 1 is the image of M33 in filter BATC07 (5785 Å), the circles in which indicate the positions of the sample clusters in this paper.

## 2.2. Observations and Data Reduction

The large field multicolor observations of the spiral galaxy M33 were obtained in the BATC photometric system. The multicolor BATC filter system, which was specifically designed to avoid contamination from the brightest and most variable night-sky emission lines, includes 15 intermediate-band filters, covering the total optical wavelength range from 3000 to 10000 Å. The images of M33 covering the whole optical body of M33 were accumulated in 13 intermediate-band filters with a total exposure time of about 32.75 hr from 1995 September 23 to 2000 August 28. The dome flat-field images were taken by using a diffuse plate in front of the correcting plate of the Schmidt telescope. For flux calibration, the Oke-Gunn primary flux standard stars HD 19445, HD 84937, BD +26°2606, and BD +17°4708 were observed during photometric nights (see details from Yan et al. 1999; Zhou et al. 2001b). Column (6) in Table 1 gives the calibration error in magnitudes for the standard stars in each filter. The formal errors we obtain for these stars in the 13 BATC filters are  $\lesssim 0.02$  mag. This indicates that we can define the standard BATC system to an accuracy of  $\lesssim 0.02$  mag.

The data were reduced with standard procedures, including bias subtraction and flat fielding of the CCD images, with an automatic data reduction software named PIPELINE I developed for the BATC multicolor sky survey (see Ma et al. 2001, 2002 for a detail).

## 2.3. Integrated Photometry

For each star cluster, the PHOT routine in DAOPHOT (Stetson 1987, 1992) is used to obtain magnitudes. For avoiding contamination from nearby objects, a smaller aperture of  $6''.8$ , which corresponds to a diameter of 4 pixels in the Ford CCDs, is adopted. Aperture corrections are computed using isolated stars. The SEDs in 13 BATC filters

for 78 star clusters were obtained. Table 2 contains the following information: Column (1) is cluster number that is taken from Chandar et al. (2001). Column (2)–(14) show the magnitudes of different bands. Second row for each star cluster is the uncertainties of the magnitudes of the corresponding bands. The uncertainties for each filter are given by DAOPHOT.

## 2.4. Comparison with Previous Photometry

Using the Landolt standards, Zhou et al. (2001a) presented the relationships between the BATC intermediate-band system and *UBVRI* broadband system from the catalogs of Landolt (1983, 1992) and Galadí-Enríquez, Trullols, & Jordi (2000). We show the coefficients of one relationship in equation (1):

$$m_V = m_{07} + (0.3233 \pm 0.019)(m_{06} - m_{08}) + 0.0590 \pm 0.010. \quad (1)$$

Using equation (1), we transformed the magnitudes of 78 star clusters in the BATC06, BATC07, and BATC08 bands to ones in the *V* band. Figure 2 plots the comparison of *V* (BATC) photometry with previously published measurements (Chandar et al. 2001). Table 3 shows this comparison. The mean *V* magnitude difference (this paper's values minus the values of Chandar et al. 2001) is  $\langle \Delta V \rangle = 0.036 \pm 0.042$ . The uncertainties in *V* (BATC) have been added linearly, i.e.,  $\sigma_B = \sigma_{07} + 0.3233(\sigma_{06} + \sigma_{08})$ , to reflect the error in the three filter measurements. From Figure 2 and Table 3, it can be seen that there is good agreement in the photometric measurements between Chandar et al. (2001) and this paper, except for clusters 115 and 127.

## 3. DATABASES OF SIMPLE STELLAR POPULATIONS

Tinsley (1972) and Searle, Sargent, & Bagnuolo (1973) did the pioneering work in evolutionary population synthesis. This method has become a standard technique for studying the stellar populations of galaxies. This is a result of the improvement in the theory of the chemical evolution of galaxies, star formation, stellar evolution and atmospheres, and of the development of synthesis algorithms, as well as the availability of various evolutionary synthesis models. A comprehensive compilation of such models was presented by Leitherer et al. (1996) and Kennicutt (1998). More widely used models are from the Padova and Geneva groups (e.g., Schaerer & de Koter 1997; Schaerer & Vacca 1998; Bressan, Chiosi, & Tantalo 1996; Chiosi et al. 1998), GISSEL96 (Charlot & Bruzual 1991; Bruzual & Charlot 1993; G. Bruzual & S. Charlot 1996, unpublished), PEGASE (Fioc & Rocca-Volmerange 1997), and STARBURST99 (Leitherer et al. 1999).

A simple stellar population (SSP) is defined as a single generation of coeval stars with fixed parameters such as metallicity, initial mass function, etc. (Buzzoni 1997). SSPs are the basic building blocks of synthetic spectra of galaxies that can be used to infer the formation and subsequent evolution of the parent galaxies (Jablonka et al. 1996). They are modeled by a collection of stellar evolutionary tracks with different masses and initial chemical compositions, supplemented with a library of stellar spectra for stars at different evolutionary stages in evolution synthesis models. In this paper, we use the SSPs of Galaxy Isochrone Synthesis Spectra Evolution Library (hereafter GSSP; G. Bruzual &

TABLE 1  
PARAMETERS OF THE BATC FILTERS AND STATISTICS OF  
OBSERVATIONS

No. (1)	Name (2)	$\lambda^a$ (Å) (3)	Exp. (hr) (4)	$N_{\text{img}}^b$ (5)	rms <sup>c</sup> (6)
1.....	BATC03	4210	00:55	04	0.024
2.....	BATC04	4546	01:05	04	0.023
3.....	BATC05	4872	03:55	19	0.017
4.....	BATC06	5250	03:19	15	0.006
5.....	BATC07	5785	04:38	17	0.011
6.....	BATC08	6075	01:26	08	0.016
7.....	BATC09	6710	01:09	08	0.006
8.....	BATC10	7010	01:41	08	0.005
9.....	BATC11	7530	02:07	10	0.017
10.....	BATC12	8000	03:00	11	0.003
11.....	BATC13	8510	03:15	11	0.005
12.....	BATC14	9170	01:15	05	0.011
13.....	BATC15	9720	05:00	26	0.009

<sup>a</sup> Central wavelength for each BATC filter.

<sup>b</sup> Image numbers for each BATC filter.

<sup>c</sup> Calibration error in magnitudes for each filter as obtained from the standard stars.

TABLE 2  
SEDs OF 78 STAR CLUSTERS

No. (1)	03 (2)	04 (3)	05 (4)	06 (5)	07 (6)	08 (7)	09 (8)	10 (9)	11 (10)	12 (11)	13 (12)	14 (13)	15 (14)
62.....	19.970	19.551	19.672	19.377	19.248	19.301	19.142	19.172	18.984	18.881	19.070	18.627	19.131
	0.238	0.186	0.168	0.162	0.133	0.168	0.151	0.188	0.180	0.166	0.268	0.187	0.389
64.....	19.433	19.262	19.282	19.171	18.988	18.984	18.969	18.891	18.837	18.848	18.735	18.646	18.524
	0.089	0.087	0.082	0.094	0.084	0.100	0.111	0.127	0.137	0.140	0.192	0.187	0.244
67.....	17.742	17.563	17.559	17.470	17.456	17.469	17.414	17.402	17.435	17.293	17.288	17.396	17.208
	0.034	0.033	0.032	0.039	0.032	0.034	0.037	0.044	0.052	0.049	0.060	0.068	0.068
68.....	17.925	17.801	17.883	17.773	17.910	17.824	17.849	17.879	17.747	17.729	17.774	17.784	17.718
	0.032	0.036	0.035	0.043	0.051	0.052	0.066	0.071	0.083	0.084	0.113	0.115	0.125
69.....	19.363	19.100	18.992	18.525	18.623	18.478	18.336	18.276	18.191	18.208	17.961	17.903	18.083
	0.154	0.125	0.135	0.155	0.100	0.088	0.093	0.087	0.099	0.103	0.106	0.102	0.163
71.....	19.640	19.258	19.241	19.131	19.054	19.065	18.974	18.977	18.887	18.928	18.931	18.535	18.705
	0.205	0.135	0.105	0.134	0.097	0.131	0.125	0.134	0.146	0.145	0.233	0.138	0.220
72.....	18.468	18.216	18.284	18.230	18.222	18.193	18.091	18.031	17.715	17.667	17.745	17.380	17.122
	0.080	0.062	0.055	0.070	0.048	0.058	0.052	0.056	0.051	0.046	0.067	0.047	0.048
73.....	20.156	19.692	19.652	19.739	19.357	19.368	19.191	19.269	19.056	18.755	19.113	18.484	18.430
	0.319	0.171	0.112	0.155	0.097	0.110	0.104	0.129	0.118	0.097	0.220	0.117	0.149
74.....	19.926	19.425	19.138	18.868	18.678	18.589	18.465	18.399	18.410	18.164	18.281	18.094	18.081
	0.201	0.142	0.095	0.100	0.064	0.069	0.064	0.068	0.072	0.061	0.098	0.076	0.101
75.....	19.782	19.400	19.256	18.811	19.164	19.177	19.370	19.133	19.033	19.028	18.796	18.969	18.790
	0.190	0.164	0.139	0.143	0.155	0.169	0.246	0.199	0.228	0.211	0.240	0.256	0.303
76.....	19.427	19.077	19.093	18.900	18.906	18.913	18.852	18.893	18.697	18.758	18.588	18.634	18.377
	0.127	0.098	0.105	0.122	0.115	0.129	0.145	0.154	0.144	0.151	0.202	0.161	0.180
77.....	18.534	18.327	18.353	18.037	18.080	17.995	17.819	17.816	17.635	17.497	17.572	17.464	17.093
	0.061	0.045	0.039	0.046	0.032	0.036	0.030	0.036	0.035	0.028	0.049	0.037	0.054
78.....	18.169	18.041	18.174	18.191	18.196	18.297	18.368	18.312	18.333	18.426	18.613	18.282	18.184
	0.065	0.064	0.064	0.090	0.066	0.092	0.100	0.110	0.124	0.104	0.225	0.114	0.175
79.....	19.398	19.123	19.082	18.970	18.831	18.799	18.789	18.665	18.516	18.452	18.258	17.980	18.000
	0.153	0.132	0.139	0.152	0.118	0.133	0.148	0.138	0.143	0.120	0.149	0.105	0.130
83.....	19.602	19.485	19.652	19.422	19.523	19.388	19.405	19.166	19.233	18.962	18.900	17.760	18.561
	0.106	0.099	0.100	0.104	0.092	0.103	0.109	0.108	0.114	0.097	0.148	0.055	0.214
84.....	20.139	20.126	20.281	20.259	19.944	20.196	20.079	20.275	20.047	20.539	20.205	20.112	19.839
	0.134	0.129	0.164	0.202	0.123	0.183	0.185	0.279	0.228	0.296	0.478	0.446	0.634
86.....	19.590	19.409	19.220	19.089	19.027	18.867	18.556	18.758	18.716	18.780	18.963	18.753	18.418
	0.107	0.087	0.073	0.070	0.056	0.056	0.072	0.065	0.067	0.083	0.163	0.108	0.153
87.....	19.913	19.440	19.219	18.963	18.888	18.684	18.533	18.450	18.497	18.348	18.188	18.234	18.276
	0.143	0.090	0.060	0.057	0.045	0.051	0.051	0.052	0.055	0.047	0.072	0.075	0.102
88.....	17.608	17.579	17.228	17.690	17.878	17.855	17.143	17.973	18.123	18.281	18.468	17.912	18.170
	0.182	0.185	0.098	0.218	0.119	0.181	0.094	0.190	0.244	0.232	0.266	0.128	0.209
89.....	18.292	18.232	18.331	18.232	18.425	18.514	17.991	18.468	18.601	18.534	18.508	18.300	18.758
	0.142	0.136	0.177	0.158	0.156	0.190	0.213	0.195	0.238	0.186	0.256	0.179	0.484
91.....	18.517	18.203	18.047	17.933	17.743	17.750	17.569	17.596	17.579	17.416	17.556	17.447	17.358
	0.092	0.074	0.060	0.056	0.042	0.045	0.051	0.042	0.046	0.043	0.059	0.062	0.076
92.....	18.876	18.707	18.755	18.590	18.589	18.481	18.469	18.433	18.515	18.378	18.535	18.376	18.353
	0.095	0.089	0.079	0.116	0.102	0.098	0.125	0.121	0.154	0.145	0.200	0.197	0.250
93.....	19.262	19.262	19.566	19.190	19.431	19.318	19.722	19.339	19.461	19.659	19.826	19.992	20.034
	0.171	0.147	0.162	0.189	0.223	0.203	0.387	0.269	0.363	0.488	0.660	0.867	1.192
94.....	18.533	18.374	18.544	18.382	18.469	18.420	18.382	18.364	18.255	18.239	18.313	18.079	18.165
	0.059	0.060	0.064	0.068	0.062	0.076	0.074	0.090	0.099	0.092	0.119	0.109	0.174
95.....	18.055	17.941	17.991	17.887	17.762	17.728	17.622	17.487	17.335	17.280	17.223	17.139	16.944
	0.040	0.038	0.036	0.041	0.038	0.041	0.042	0.039	0.041	0.042	0.046	0.045	0.054
96.....	19.486	19.442	19.451	19.457	19.432	19.473	19.164	19.234	19.361	19.148	19.002	18.754	19.249
	0.145	0.163	0.147	0.181	0.183	0.219	0.187	0.212	0.269	0.228	0.257	0.181	0.459
97.....	19.183	18.805	18.641	18.486	18.293	18.168	17.825	17.793	17.723	17.607	17.532	17.369	17.444
	0.125	0.105	0.091	0.086	0.067	0.068	0.063	0.059	0.069	0.057	0.065	0.056	0.094
99.....	19.015	18.739	18.673	18.494	18.342	18.363	18.321	18.171	17.915	17.816	17.880	17.670	17.328
	0.204	0.185	0.167	0.179	0.146	0.181	0.226	0.199	0.167	0.145	0.192	0.164	0.146
100.....	17.161	17.057	17.137	17.160	17.172	17.307	17.342	17.371	17.529	17.575	17.569	17.901	18.167
	0.036	0.039	0.043	0.052	0.049	0.059	0.099	0.085	0.113	0.120	0.141	0.207	0.339
101.....	19.580	19.227	19.624	19.130	19.019	19.071	19.863	19.110	19.108	18.962	19.296	19.319	18.789
	0.414	0.344	0.431	0.343	0.282	0.326	0.899	0.448	0.524	0.442	0.677	0.715	0.623
103.....	19.482	19.223	19.071	18.870	18.764	18.713	19.007	18.876	19.205	18.948	18.872	19.680	20.271
	0.354	0.321	0.257	0.259	0.218	0.225	0.418	0.333	0.528	0.422	0.438	0.945	2.321
107.....	18.788	18.541	18.507	18.462	18.378	18.395	18.229	18.273	18.119	18.037	18.070	18.003	17.890
	0.070	0.059	0.049	0.060	0.044	0.049	0.053	0.058	0.059	0.061	0.084	0.084	0.119

TABLE 2—Continued

No. (1)	03 (2)	04 (3)	05 (4)	06 (5)	07 (6)	08 (7)	09 (8)	10 (9)	11 (10)	12 (11)	13 (12)	14 (13)	15 (14)
108 .....	19.316	19.304	19.268	19.017	19.215	19.055	19.091	19.046	18.948	18.775	18.952	18.904	18.524
	0.188	0.178	0.124	0.140	0.133	0.118	0.151	0.152	0.146	0.140	0.212	0.174	0.200
109 .....	17.991	17.778	17.812	17.777	17.727	17.726	17.692	17.658	17.605	17.498	17.608	17.392	17.472
	0.049	0.044	0.042	0.054	0.044	0.054	0.053	0.058	0.063	0.056	0.074	0.059	0.090
110 .....	19.262	18.791	18.784	18.594	18.506	18.497	18.480	18.440	18.391	18.358	18.232	18.295	18.385
	0.087	0.067	0.057	0.048	0.048	0.046	0.052	0.055	0.066	0.073	0.083	0.086	0.190
112 .....	19.082	18.794	18.735	18.508	18.485	18.396	18.330	18.332	18.221	18.036	18.078	18.071	18.168
	0.082	0.071	0.059	0.063	0.053	0.056	0.059	0.065	0.071	0.063	0.080	0.082	0.161
113 .....	19.868	19.545	19.527	19.685	19.362	19.618	19.706	19.577	19.689	19.498	19.968	20.229	20.099
	0.109	0.074	0.068	0.089	0.066	0.083	0.101	0.122	0.146	0.142	0.324	0.438	0.812
115 .....	17.867	17.660	17.796	17.740	17.836	17.857	17.920	17.798	17.940	17.874	17.975	17.971	17.635
	0.023	0.018	0.018	0.020	0.019	0.023	0.027	0.029	0.038	0.039	0.055	0.063	0.078
117 .....	19.060	18.904	18.837	18.710	18.726	18.790	18.718	18.741	18.765	18.636	18.809	18.355	18.748
	0.164	0.160	0.132	0.149	0.156	0.177	0.196	0.213	0.252	0.228	0.362	0.253	0.433
118 .....	18.322	18.002	17.883	17.658	17.515	17.387	17.274	17.129	17.049	17.104	16.974	16.722	16.782
	0.163	0.154	0.123	0.126	0.091	0.094	0.087	0.084	0.084	0.084	0.089	0.066	0.089
119 .....	18.481	18.162	18.088	17.866	17.719	17.599	17.540	17.336	17.262	17.306	17.163	16.898	16.947
	0.160	0.154	0.122	0.126	0.093	0.094	0.096	0.082	0.086	0.081	0.086	0.063	0.089
120 .....	18.281	17.983	18.108	18.002	18.041	18.003	18.165	18.019	18.252	18.369	18.309	19.015	19.853
	0.261	0.236	0.234	0.280	0.234	0.276	0.309	0.308	0.427	0.429	0.470	0.904	2.539
121 .....	18.602	18.290	18.297	18.184	18.466	18.422	17.962	18.808	19.161	19.213	19.548	19.123	20.396
	0.189	0.148	0.139	0.137	0.147	0.154	0.189	0.221	0.370	0.412	0.739	0.600	2.042
122 .....	17.297	17.137	17.189	17.132	17.025	17.054	17.125	17.010	17.031	16.954	16.881	16.804	16.758
	0.165	0.145	0.129	0.144	0.096	0.123	0.200	0.155	0.186	0.134	0.146	0.135	0.191
124 .....	18.820	18.849	19.003	18.906	19.068	19.208	19.177	19.057	18.998	19.262	19.231	19.251	18.488
	0.144	0.161	0.155	0.173	0.163	0.208	0.218	0.194	0.189	0.276	0.293	0.324	0.239
125 .....	18.412	18.348	18.463	18.429	18.485	18.500	18.520	18.491	18.812	18.746	18.457	18.364	18.855
	0.134	0.157	0.160	0.192	0.183	0.220	0.258	0.273	0.423	0.368	0.309	0.277	0.588
126 .....	20.649	19.648	19.545	19.327	18.988	18.935	19.072	18.551	18.416	18.252	18.116	17.992	18.019
	0.876	0.393	0.362	0.366	0.223	0.235	0.312	0.190	0.188	0.151	0.153	0.146	0.181
127 .....	15.712	15.650	15.796	15.767	15.971	15.950	15.990	15.966	15.994	16.108	16.167	16.250	16.078
	0.035	0.037	0.038	0.044	0.065	0.070	0.104	0.095	0.104	0.107	0.126	0.139	0.148
128 .....	18.885	18.545	18.441	18.464	18.246	18.375	18.286	18.155	17.886	17.819	17.829	17.690	17.531
	0.429	0.352	0.268	0.367	0.263	0.342	0.327	0.330	0.298	0.268	0.291	0.281	0.296
129 .....	18.234	18.107	18.174	18.193	17.865	18.039	18.037	17.910	17.675	17.642	17.357	17.286	17.284
	0.204	0.214	0.203	0.280	0.159	0.235	0.276	0.261	0.236	0.213	0.167	0.177	0.204
130 .....	17.671	17.323	17.481	17.221	17.431	17.063	16.851	16.810	16.780	17.125	16.663	16.678	16.598
	0.089	0.078	0.079	0.089	0.087	0.080	0.066	0.075	0.086	0.114	0.087	0.093	0.108
131 .....	18.270	17.870	17.868	17.746	17.539	17.479	17.316	17.315	17.320	17.336	17.205	17.238	17.084
	0.113	0.089	0.074	0.079	0.052	0.054	0.049	0.052	0.061	0.058	0.069	0.077	0.085
132 .....	18.892	18.955	18.947	18.861	18.929	18.856	18.697	18.647	18.495	18.548	18.492	18.581	18.247
	0.211	0.216	0.187	0.203	0.170	0.174	0.176	0.182	0.172	0.180	0.227	0.256	0.256
133 .....	18.650	18.490	18.531	18.497	18.402	18.395	18.242	18.170	18.113	18.064	17.988	17.981	17.860
	0.123	0.127	0.124	0.162	0.117	0.135	0.123	0.124	0.127	0.114	0.136	0.127	0.157
135 .....	19.484	19.079	19.000	19.412	19.010	18.905	18.500	18.947	18.643	18.708	18.632	18.785	18.347
	0.355	0.290	0.226	0.425	0.236	0.220	0.153	0.258	0.188	0.248	0.261	0.356	0.294
136 .....	19.374	19.079	19.099	18.960	18.877	18.905	18.869	18.865	18.835	18.719	18.731	18.949	18.561
	0.213	0.216	0.201	0.236	0.187	0.224	0.205	0.242	0.258	0.221	0.275	0.342	0.303
137 .....	18.374	18.095	18.196	18.136	18.121	18.130	18.066	18.137	18.138	18.090	18.139	17.906	18.133
	0.072	0.065	0.067	0.074	0.064	0.075	0.082	0.090	0.103	0.101	0.140	0.106	0.188
139 .....	18.633	18.520	18.578	18.535	18.458	18.413	18.351	18.317	18.227	18.332	18.352	17.962	18.158
	0.069	0.062	0.063	0.066	0.056	0.061	0.067	0.069	0.072	0.082	0.116	0.079	0.149
141 .....	16.069	15.987	16.128	16.155	16.240	16.306	16.371	16.357	16.419	16.395	16.284	16.346	16.396
	0.033	0.043	0.041	0.051	0.041	0.052	0.078	0.064	0.075	0.067	0.071	0.071	0.094
142 .....	15.743	15.699	15.809	15.800	15.863	15.856	15.761	15.617	15.451	15.305	15.310	15.184	14.932
	0.012	0.011	0.010	0.014	0.010	0.011	0.012	0.010	0.009	0.007	0.009	0.008	0.009
144 .....	19.991	19.810	19.717	19.464	19.386	19.214	18.917	19.089	19.036	19.060	19.145	19.179	19.271
	0.280	0.216	0.187	0.175	0.124	0.123	0.125	0.143	0.130	0.126	0.239	0.206	0.391
145 .....	20.109	19.798	19.680	19.592	19.385	19.249	19.422	19.360	19.483	19.586	19.931	19.743	21.150
	0.255	0.202	0.169	0.188	0.136	0.141	0.179	0.192	0.238	0.285	0.452	0.431	2.438
146 .....	18.574	18.249	18.294	18.135	18.350	18.303	18.350	18.470	18.363	18.436	18.446	18.493	18.114
	0.278	0.245	0.235	0.272	0.246	0.273	0.393	0.357	0.387	0.358	0.432	0.426	0.328
147 .....	18.439	18.360	18.441	18.356	18.420	18.419	18.328	18.393	18.521	18.541	18.809	18.709	18.733
	0.033	0.031	0.027	0.027	0.026	0.033	0.031	0.042	0.046	0.060	0.134	0.100	0.181
148 .....	18.016	17.901	17.520	18.051	18.136	18.184	17.009	18.122	18.111	18.200	18.618	17.935	18.093

TABLE 2—Continued

No. (1)	03 (2)	04 (3)	05 (4)	06 (5)	07 (6)	08 (7)	09 (8)	10 (9)	11 (10)	12 (11)	13 (12)	14 (13)	15 (14)
150.....	0.076	0.072	0.041	0.068	0.072	0.081	0.040	0.108	0.119	0.130	0.238	0.134	0.207
	17.541	17.380	17.432	17.361	17.408	17.432	17.426	17.410	17.444	17.470	17.575	17.479	17.491
	0.064	0.062	0.053	0.070	0.067	0.079	0.085	0.093	0.104	0.101	0.128	0.119	0.147
151.....	17.717	17.493	17.502	17.390	17.333	17.305	17.257	17.200	17.152	17.097	17.067	16.968	16.941
	0.063	0.063	0.055	0.067	0.054	0.061	0.062	0.062	0.064	0.059	0.068	0.063	0.080
152.....	19.190	18.928	18.904	18.942	18.840	18.901	18.746	18.870	18.701	18.730	18.806	18.683	18.534
	0.137	0.130	0.128	0.156	0.125	0.148	0.145	0.177	0.163	0.171	0.249	0.206	0.264
153.....	18.949	18.733	18.681	18.616	18.538	18.549	18.387	18.491	18.573	18.362	18.095	18.405	18.038
	0.132	0.129	0.125	0.116	0.105	0.104	0.141	0.113	0.139	0.126	0.127	0.175	0.162
154.....	17.890	17.734	17.789	17.698	17.718	17.713	17.575	17.611	17.569	17.512	17.407	17.338	17.323
	0.045	0.041	0.040	0.045	0.040	0.047	0.066	0.055	0.067	0.062	0.067	0.062	0.107
155.....	17.677	17.509	17.548	17.530	17.478	17.503	17.501	17.539	17.504	17.467	17.533	17.428	17.529
	0.030	0.028	0.028	0.036	0.032	0.036	0.041	0.049	0.058	0.057	0.083	0.076	0.103
156.....	18.492	18.356	18.375	18.248	18.267	18.233	18.327	18.297	18.387	18.350	18.244	18.218	18.651
	0.101	0.111	0.102	0.116	0.104	0.109	0.132	0.135	0.153	0.149	0.171	0.164	0.282
157.....	20.023	19.557	19.483	19.239	19.180	19.180	19.181	19.103	19.149	19.052	19.202	19.499	18.769
	0.401	0.310	0.247	0.264	0.210	0.229	0.258	0.247	0.303	0.266	0.370	0.532	0.301
158.....	15.950	15.913	15.947	16.070	16.158	16.146	15.869	16.074	15.849	15.869	15.813	15.508	15.466
	0.044	0.050	0.045	0.065	0.051	0.058	0.057	0.059	0.055	0.048	0.054	0.043	0.046
159.....	16.699	16.684	16.909	16.777	17.034	16.943	16.937	16.984	16.903	17.134	16.907	16.910	16.877
	0.034	0.032	0.035	0.036	0.035	0.036	0.056	0.049	0.052	0.056	0.063	0.064	0.083
160.....	18.762	18.558	18.638	18.565	18.521	18.452	18.495	18.332	18.366	18.334	18.042	18.183	18.043
	0.098	0.088	0.082	0.091	0.072	0.079	0.098	0.082	0.090	0.091	0.110	0.119	0.135
161.....	19.364	19.028	18.869	18.660	18.457	18.339	18.180	18.074	17.956	17.942	17.951	17.631	17.631
	0.077	0.054	0.039	0.034	0.033	0.033	0.034	0.036	0.035	0.038	0.059	0.043	0.078
162.....	20.196	20.274	20.054	19.939	19.828	19.798	19.283	19.342	19.375	19.258	19.030	19.141	18.773
	0.130	0.106	0.095	0.089	0.078	0.087	0.097	0.080	0.089	0.087	0.143	0.135	0.168

S. Charlot 1996, unpublished) to estimate the ages of the sample clusters, since they are simple and reasonably well understood.

### 3.1. SED of GSSPs

Charlot & Bruzual (1991) developed a model of stellar population synthesis. In this model, the population synthesis method can be used to determine the distribution of stars in the theoretical color-magnitude diagram for any stellar

system. Bruzual & Charlot (1993) presented “isochrone synthesis” as a natural and reliable approach for modeling the evolution of stellar populations in star clusters and galaxies. With this isochrone synthesis algorithm, Bruzual & Charlot (1993) computed the SEDs of stellar populations with solar metallicity. G. Bruzual & S. Charlot (1996, unpublished) improved the Bruzual & Charlot (1993) evolutionary population synthesis models. The updated version provides the evolution of the spectrophotometric properties for a wide range of stellar metallicity, which are  $Z = 0.0004, 0.004, 0.008, 0.02, 0.05, \text{ and } 0.1$  (see Ma et al. 2001, 2002 for details).

### 3.2. Integrated Colors of GSSPs

Kong et al. (2000) have obtained the age, metallicity, and interstellar medium reddening distribution for M81. They found the best match between the intrinsic colors and the predictions of GSSP for each cell of M81. To estimate the ages for the sample clusters in this paper, we follow the method of Kong et al. (2000). As we know, the observational data are integrated luminosities. As a result, we need to convolve the SED of GSSP with BATC filter profiles to obtain the optical and near-infrared integrated luminosities for comparison (Kong et al. 2000). The integrated luminosity  $L_{\lambda_i}(t, Z)$  of the  $i$ th BATC filter can be calculated with

$$L_{\lambda_i}(t, Z) = \frac{\int F_{\lambda}(t, Z)\varphi_i(\lambda)d\lambda}{\int \varphi_i(\lambda)d\lambda}, \quad (2)$$

where  $F_{\lambda}(t, Z)$  is the SED of the GSSP of metallicity  $Z$  at age  $t$ , and  $\varphi_i(\lambda)$  is the response function of the  $i$ th filter of the BATC filter system ( $i = 3, 4, \dots, 15$ ), respectively. For avoiding to use the parameters that are dependent on the

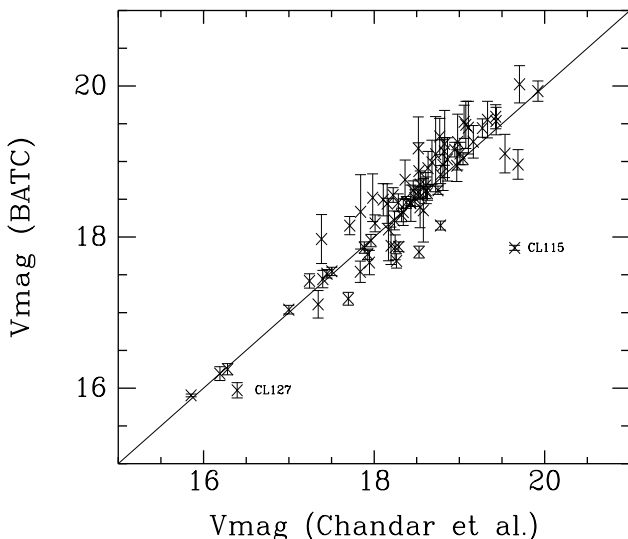


FIG. 2.—Comparison of cluster photometry with previous measurements (HST).

TABLE 3  
COMPARISON OF CLUSTER PHOTOMETRY WITH PREVIOUS MEASUREMENTS

$V$			$V$		
No.	(Chandar et al.)	$V$ (BATC)	No.	(Chandar et al.)	$V$ (BATC)
62.....	18.769 ± 0.005	19.332 ± 0.240	118.....	17.945 ± 0.005	17.662 ± 0.162
64.....	19.007 ± 0.008	19.107 ± 0.147	119.....	18.247 ± 0.006	17.864 ± 0.164
67.....	17.446 ± 0.002	17.515 ± 0.056	120.....	18.169 ± 0.000	18.100 ± 0.414
68.....	17.963 ± 0.003	17.953 ± 0.082	121.....	18.431 ± 0.010	18.448 ± 0.241
69.....	18.541 ± 0.005	18.697 ± 0.179	122.....	17.343 ± 0.004	17.109 ± 0.182
71.....	18.822 ± 0.004	19.134 ± 0.183	124.....	18.859 ± 0.009	19.029 ± 0.286
72.....	18.321 ± 0.003	18.293 ± 0.089	125.....	17.983 ± 0.005	18.521 ± 0.316
73.....	19.430 ± 0.007	19.536 ± 0.183	126.....	18.518 ± 0.007	19.174 ± 0.417
74.....	18.780 ± 0.003	18.827 ± 0.119	127.....	16.394 ± 0.003	15.971 ± 0.102
75.....	19.534 ± 0.007	19.105 ± 0.256	128.....	17.841 ± 0.010	18.334 ± 0.492
76.....	19.687 ± 0.000	18.961 ± 0.196	129.....	17.383 ± 0.006	17.974 ± 0.325
77.....	18.778 ± 0.003	18.153 ± 0.059	130.....	17.838 ± 0.006	17.541 ± 0.142
78.....	18.238 ± 0.003	18.221 ± 0.125	131.....	18.262 ± 0.007	17.684 ± 0.095
79.....	18.969 ± 0.005	18.945 ± 0.210	132.....	18.678 ± 0.014	18.990 ± 0.292
83.....	19.426 ± 0.006	19.593 ± 0.159	133.....	18.106 ± 0.006	18.494 ± 0.213
84.....	19.705 ± 0.006	20.023 ± 0.247	135.....	18.826 ± 0.013	19.233 ± 0.445
86.....	18.945 ± 0.004	19.158 ± 0.097	136.....	18.807 ± 0.011	18.954 ± 0.336
87.....	19.041 ± 0.006	19.037 ± 0.080	137.....	18.011 ± 0.006	18.182 ± 0.112
88.....	18.198 ± 0.003	17.884 ± 0.248	139.....	18.223 ± 0.004	18.556 ± 0.097
89.....	18.538 ± 0.004	18.393 ± 0.269	141.....	16.281 ± 0.002	16.250 ± 0.074
91.....	17.886 ± 0.003	17.861 ± 0.075	142.....	15.854 ± 0.001	15.904 ± 0.018
92.....	18.605 ± 0.008	18.683 ± 0.171	144.....	19.055 ± 0.014	19.526 ± 0.220
93.....	19.105 ± 0.014	19.449 ± 0.350	145.....	19.329 ± 0.016	19.555 ± 0.242
94.....	18.478 ± 0.005	18.516 ± 0.109	146.....	18.577 ± 0.012	18.355 ± 0.422
95.....	18.289 ± 0.004	17.872 ± 0.065	147.....	18.423 ± 0.007	18.459 ± 0.045
96.....	19.075 ± 0.009	19.486 ± 0.312	148.....	17.714 ± 0.006	18.152 ± 0.120
97.....	18.283 ± 0.006	18.455 ± 0.117	150.....	17.398 ± 0.004	17.444 ± 0.115
99.....	18.154 ± 0.006	18.443 ± 0.262	151.....	17.242 ± 0.004	17.419 ± 0.095
100.....	17.697 ± 0.007	17.183 ± 0.085	152.....	18.632 ± 0.009	18.912 ± 0.223
101.....	18.721 ± 0.012	19.097 ± 0.498	153.....	18.610 ± 0.009	18.619 ± 0.176
103.....	18.525 ± 0.011	18.874 ± 0.374	154.....	17.924 ± 0.005	17.772 ± 0.070
107.....	18.378 ± 0.003	18.459 ± 0.079	155.....	17.504 ± 0.003	17.546 ± 0.055
108.....	19.162 ± 0.006	19.262 ± 0.216	156.....	18.341 ± 0.008	18.331 ± 0.177
109.....	18.527 ± 0.000	17.802 ± 0.079	157.....	18.979 ± 0.012	19.258 ± 0.369
110.....	18.515 ± 0.003	18.596 ± 0.078	158.....	16.191 ± 0.002	16.192 ± 0.091
112.....	18.625 ± 0.004	18.580 ± 0.091	159.....	17.000 ± 0.003	17.039 ± 0.058
113.....	19.269 ± 0.006	19.443 ± 0.122	160.....	18.458 ± 0.007	18.617 ± 0.127
115.....	19.648 ± 0.007	17.857 ± 0.033	161.....	18.749 ± 0.005	18.620 ± 0.055
117.....	18.363 ± 0.006	18.759 ± 0.261	162.....	19.920 ± 0.014	19.933 ± 0.135

distance. We calculate the integrated colors of a GSSP relative to the BATC filter BATC08 ( $\lambda = 6075 \text{ \AA}$ ):

$$C_{\lambda_i}(t, Z) = L_{\lambda_i}(t, Z)/L_{6075}(t, Z). \quad (3)$$

As a result, we obtained the intermediate-band colors of a GSSP for six metallicities from  $Z = 0.0004$  to  $0.1$  using equations (2) and (3).

#### 4. AGE ESTIMATES

In order to obtain intrinsic colors of 78 clusters and hence accurate ages the photometric measurements must be dereddened. As Chandar et al. (2001) did, we adopted  $E(B-V) = 0.10$ . In addition, we adopted the extinction curve presented by Zombeck (1990). An extinction correction  $A_\lambda = R_\lambda E(B-V)$  was applied; here  $R_\lambda$  is obtained by interpolating using the data of Zombeck (1990).

Since we model the stellar populations of the star clusters by SSPs, the intrinsic colors for each star cluster are determined by two parameters: age and metallicity. We will determine the ages and best-fitted models of metallicity for these star clusters simultaneously by a least-squares method. The age and best-fitted model of metallicity are found by minimizing the difference between the intrinsic and integrated colors of GSSP:

$$R^2(n, t, Z) = \sum_{i=3}^{15} [C_{\lambda_i}^{\text{intr}}(n) - C_{\lambda_i}^{\text{ssp}}(t, Z)]^2, \quad (4)$$

where  $C_{\lambda_i}^{\text{ssp}}(t, Z)$  represents the integrated color in the  $i$ th filter of a SSP at age  $t$  in the model of metallicity  $Z$  and  $C_{\lambda_i}^{\text{intr}}(n)$  is the intrinsic integrated color for  $n$ th star cluster. Using the stellar evolutionary models (Bertelli et al. 1994) and published line indices of 22 M33 older clusters, Chandar et al. (1999b) narrowed the range of cluster metallicities ( $Z$ ) to be from  $\sim 0.0002$  to  $0.03$ . As a result, we only select

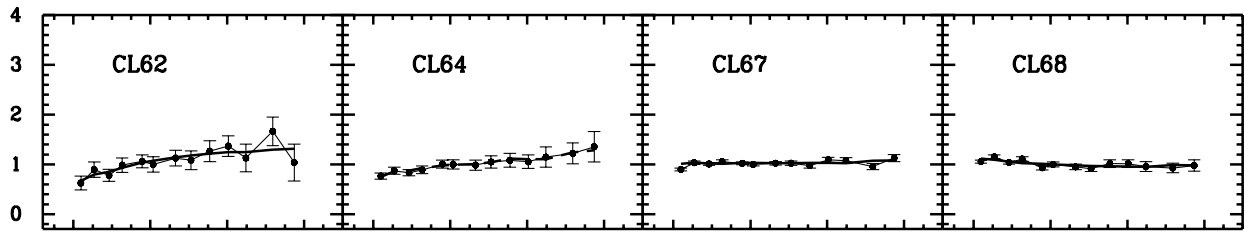


FIG. 3.—Map of the best fit of the integrated color of a SSP with intrinsic integrated color for 78 star clusters. The thick line represents the integrated color of a SSP, and the filled circle represents the intrinsic integrated color of a star cluster.

the models of three metallicities, 0.0004, 0.004, and 0.02 from GSSP.

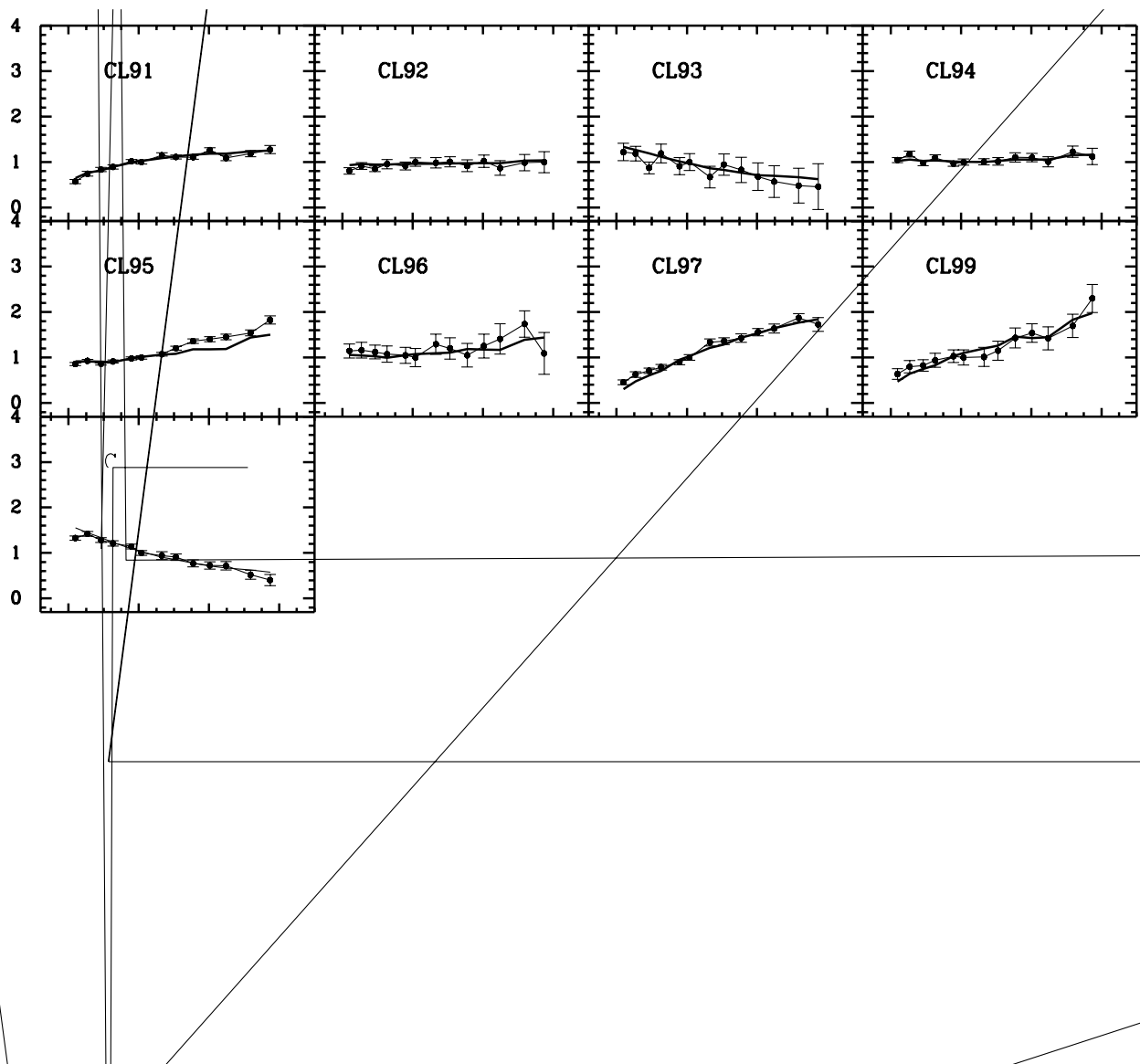
Figure 3 shows the map of the best fit of the integrated color of a SSP with the intrinsic integrated color for 78 star clusters, and Table 4 presents the best-fitted models of metallicities and ages for these star clusters. In Figure 3, the thick line represents the integrated color of a SSP of GSSP, and the filled circle represents the intrinsic integrated color of a star cluster. From this figure, we see that clusters 83, 88, and 148 have strong emission lines. In the process of fitting, we did not use the strong emission lines.

Figure 4 presents a histogram of cluster ages. The results show that, in general, M33 clusters have been forming continuously, with ages of  $\sim 3 \times 10^6$ – $10^{10}$  yr. This conclusion confirms the results of Chandar, Bianchi, & Ford (2001). There exist three groups of clusters that formed with three models of metallicities,  $Z = 0.02$ , 0.004, and 0.0004. In dif-

ferent models of metallicities, the distribution of cluster ages is a little different too. In the model of  $Z = 0.02$ , the ages of most clusters are younger than  $\sim 10^9$  yr, and there are two peaks at  $\sim 10^7$  and  $\sim 10^9$  yr. In the model of  $Z = 0.004$ , the clusters formed from  $\sim 3 \times 10^6$  to  $10^{10}$  yr, and the distribution of ages is more homogeneous than in the other two models. In the model of  $Z = 0.0004$ , the most clusters formed from  $\sim 10^8$  to  $10^{10}$  yr. Clusters 97, 106, and 162 have derived ages consistent with that of the globular clusters of the Milky Way,  $\sim 1.5 \times 10^{10}$  yr. This result is also consistent with that found by Chandar, Bianchi, & Ford (1999b) and Ma et al. (2001), who presented clusters 11, 28, 29, and 57 to be as old as  $\sim 1.5 \times 10^{10}$  yr.

In this section, we estimate the ages of our sample clusters by comparing the photometry of each object with the theoretical stellar population synthesis models for different values of metallicity. However, we want to emphasize that, for





clusters older than several  $10^8$  yr, the age/metallicity degeneracy becomes pronounced. In this case, we only mean that in some models of metallicity, the intrinsic integrated color of a cluster can give the best fit with the integrated color of a SSP at some age. In addition, the uncertainties in the age estimates arising from photometric uncertainties are 0.2 or so, i.e.,  $\text{age} \pm 0.2 \times \text{age}$  (log yr).

## 5. SUMMARY AND DISCUSSION

In this paper, we have, for the first time, obtained the SEDs of 78 star clusters of M33 in 13 intermediate colors with the BAO 60/90 cm Schmidt telescope. Below, we summarize our main conclusions.

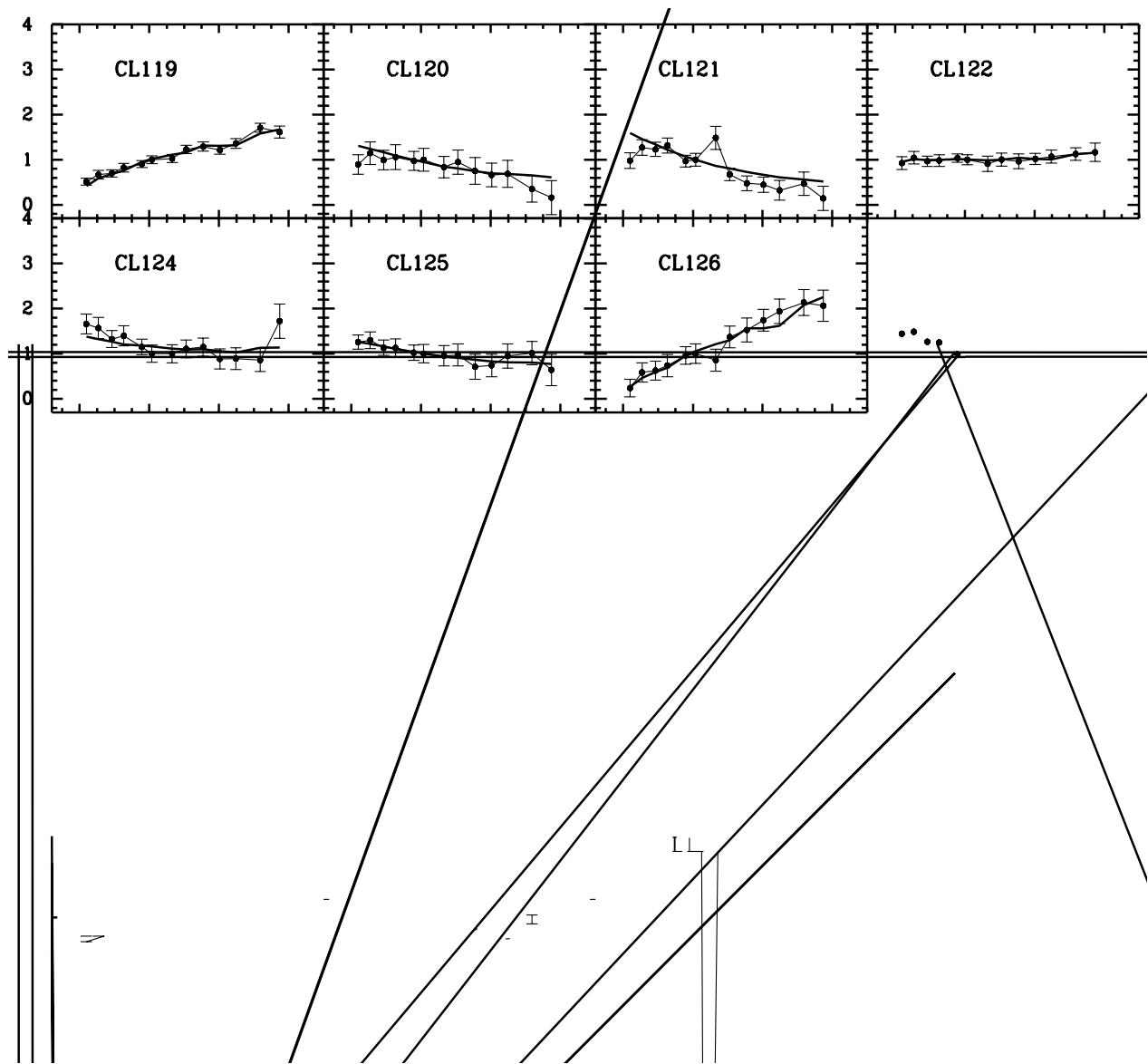
1. Using the images obtained with the BAO 60/90 cm Schmidt telescope in 13 intermediate-band filters from 3800 to 10000 Å, we obtained the SEDs of 78 star clusters that were detected by Chandar et al. (2001).

2. By comparing the integrated photometric measurements with theoretical stellar population synthesis models,

we find that clusters formed continuously in M33 from  $\sim 3 \times 10^6$  to  $10^{10}$  yr. The results also show that there are two peaks at  $\sim 8 \times 10^6$  and  $\sim 10^9$  yr.

Chandar et al. (1999a, 1999b) estimated ages for 60 star clusters in M33 by comparing the photometric measurements to integrated color from theoretical models by Bertelli et al. (1994). Their results showed that the integrated colors of star clusters depend mostly on age, with a secondary dependence on chemical composition. As a result, we can estimate ages of clusters but cannot determine metallicities of clusters exactly. As Chandar, Bianchi, & Ford (1999b, 2001) and Chandar et al. (1999c) did, we also estimated the ages of our sample clusters by comparing the photometry of each object with models for different values of metallicity. Although we presented the metallicity of each cluster in Table 4, we only mean that, in this model of metallicity, the intrinsic integrated color of each cluster can do the best fit with the integrated color of a SSP.

With spectrophotometry, Christian & Schommer (1983) obtained the ages of the star clusters in M33 to be  $\sim 10^7$ – $10^{10}$



yr. Using the integrated *UBV* photometry and *IUE*  $\lambda\lambda 1200\text{--}3000$  spectra, Ciani, D’Odorico, & Benvenuti (1984) studied the minuscule “bulge” population of M33 and found that a multigeneration model, where a young component (age of  $\sim 10^7$  yr) and an old, metal-poor one (age of  $\sim 5 \times 10^9$  yr) are superposed, gives the best fit to the observed data. Schmidt, Bica, & Alloin (1990) applied a population synthesis method that uses a star cluster spectral library and a grid of the star cluster spectral properties as a function of age and metallicity (Bica & Alloin 1986a, 1986b; 1987) to the bluish nucleus of M33 and gave an age of less than  $5 \times 10^8$  yr for the dominant blue bulge population. From the histogram of ages in this paper, we can see that some old clusters in our sample appear to be coeval with the old population of the bulge.

We would like to thank the anonymous referee for his or her insightful comments and suggestions that improved this paper. We are grateful to the Padova group for providing us with a set of theoretical isochrones and SSPs. We also thank G. Bruzual and S. Charlot for sending us their latest calculations of SSPs and for explanations of their code. The work is supported partly by the National Sciences Foundation under the contract Nos. 19833020 and 19503003. The BATC survey is supported by the Chinese Academy of Sciences, the Chinese National Natural Science Foundation, and the Chinese State Committee of Sciences and Technology. The project is also supported in part by the National Science Foundation (grant INT 93-01805) and by Arizona State University, the University of Arizona, and Western Connecticut State University.

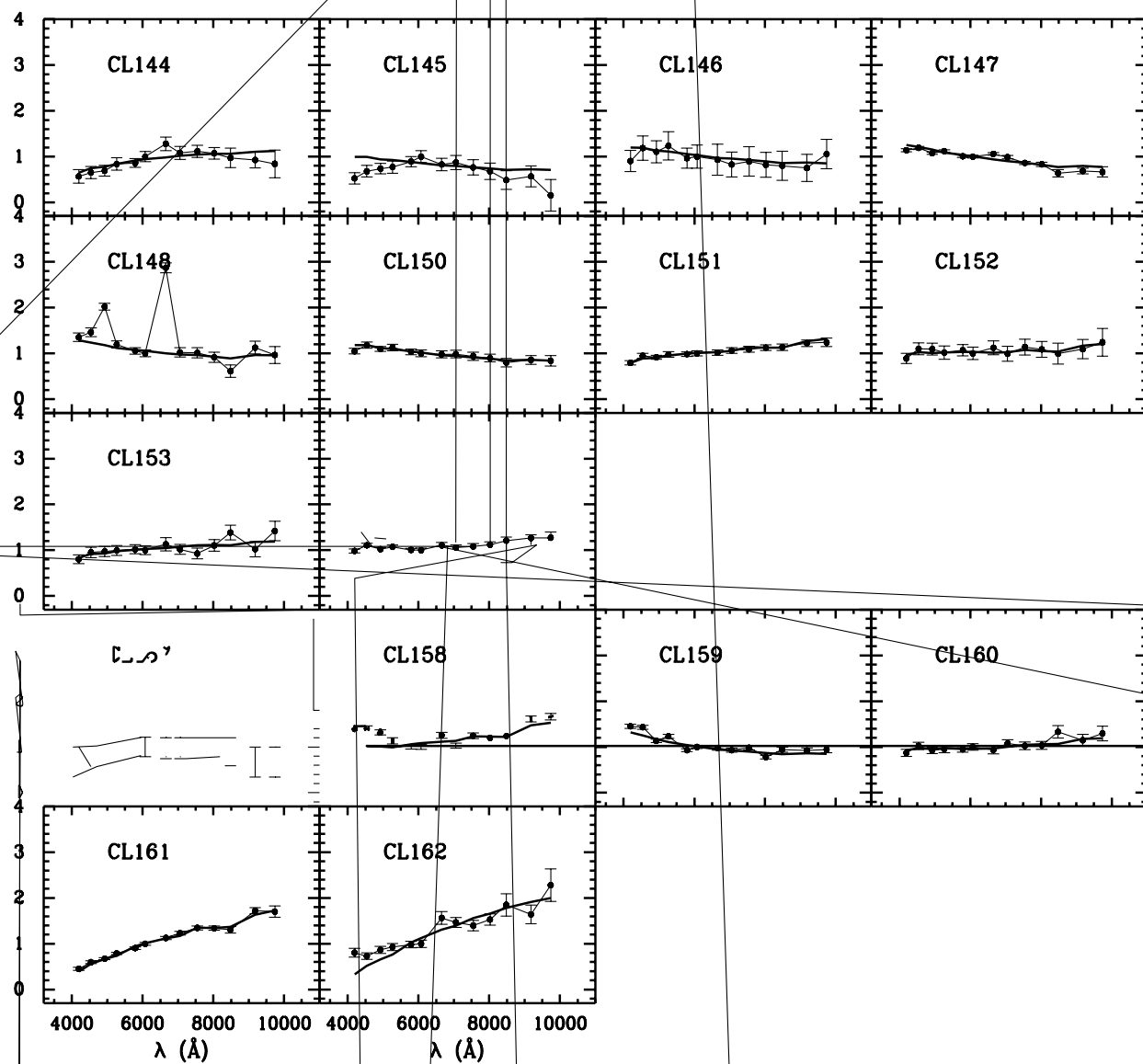


FIG. 3.—Continued

TABLE 4  
AGE DISTRIBUTION OF 78 STAR CLUSTERS

No.	Metallicity (Z)	Age (log yr)	No.	Metallicity (Z)	Age (log yr)
62.....	0.00040	9.279	118.....	0.02000	9.155
64.....	0.00400	8.806	119.....	0.02000	9.155
67.....	0.00400	7.720	120.....	0.00400	6.600
68.....	0.00400	7.021	121.....	0.02000	6.620
69.....	0.00040	9.760	122.....	0.00400	8.307
71.....	0.02000	8.606	124.....	0.02000	6.860
72.....	0.02000	9.107	125.....	0.00400	6.860
73.....	0.02000	9.107	126.....	0.02000	9.954
74.....	0.00400	9.322	127.....	0.00040	7.220
75.....	0.00040	8.757	128.....	0.00400	9.107
76.....	0.00400	8.757	129.....	0.02000	6.940
77.....	0.02000	9.009	130.....	0.00400	9.057
78.....	0.02000	6.800	131.....	0.00040	9.301
79.....	0.02000	9.107	132.....	0.02000	6.980
83.....	0.02000	6.940	133.....	0.02000	6.960
84.....	0.02000	6.860	135.....	0.02000	6.940
86.....	0.00040	9.155	136.....	0.00040	8.806
87.....	0.00040	10.061	137.....	0.02000	8.057
88.....	0.00400	6.480	139.....	0.02000	7.179
89.....	0.00040	6.580	141.....	0.00040	6.660
91.....	0.00040	9.255	142.....	0.02000	6.940
92.....	0.00400	7.699	144.....	0.00040	9.107
93.....	0.00400	6.600	145.....	0.00040	8.009
94.....	0.00040	8.356	146.....	0.00040	8.009
95.....	0.02000	6.940	147.....	0.02000	6.760
96.....	0.02000	6.920	148.....	0.02000	6.840
97.....	0.00400	10.279	150.....	0.00040	8.009
99.....	0.02000	9.107	151.....	0.00400	8.757
100.....	0.02000	6.680	152.....	0.00400	8.356
101.....	0.02000	8.057	153.....	0.00040	8.906
103.....	0.00400	6.620	154.....	0.00040	8.507
107.....	0.00400	8.857	155.....	0.00400	6.960
108.....	0.00400	8.507	156.....	0.00040	8.009
109.....	0.00040	8.657	157.....	0.00040	8.957
110.....	0.00040	8.957	158.....	0.02000	6.980
112.....	0.00040	9.207	159.....	0.00400	7.179
113.....	0.00040	7.806	160.....	0.00040	8.507
115.....	0.02000	6.840	161.....	0.02000	9.225
117.....	0.00400	8.009	162.....	0.00400	10.283

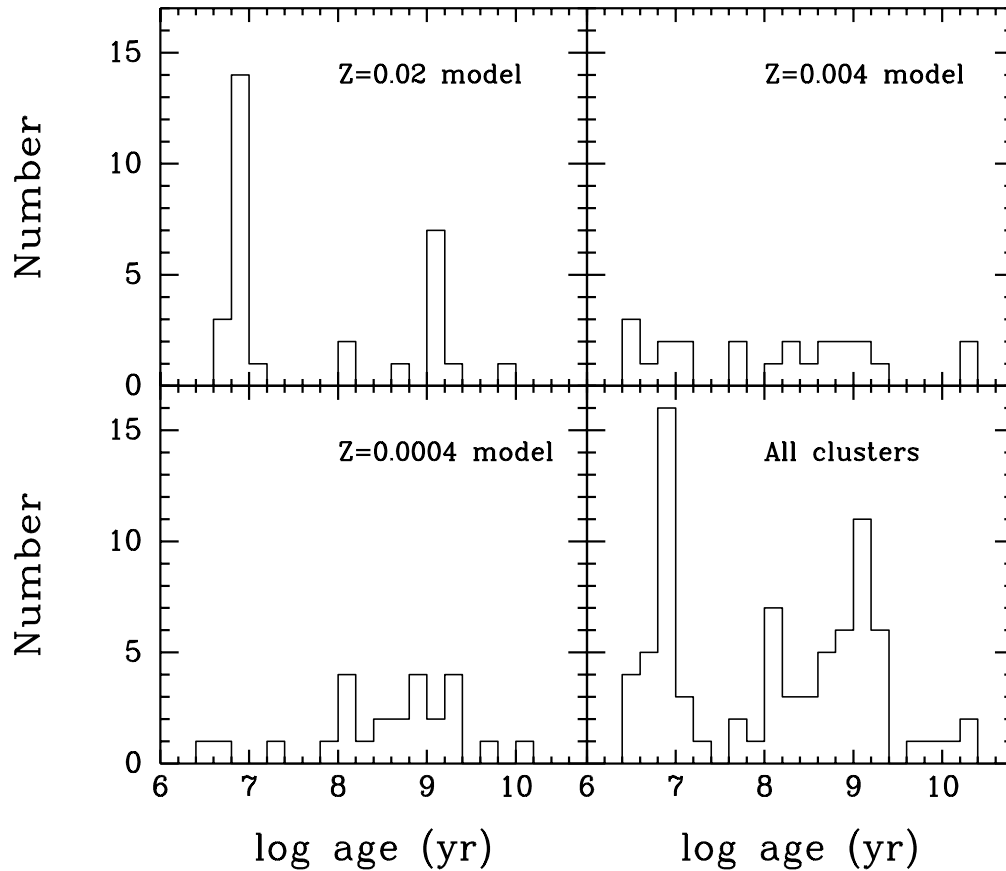


FIG. 4.—Histogram of M33 cluster ages

## REFERENCES

- Bertelli, O., Bressan, A., Chiosi, C., Fagotto, F., & Nasi, E. 1994, *A&AS*, 106, 275
- Bica, E., & Alloin, D. 1986a, *A&A*, 162, 21
- . 1986b, *A&AS*, 66, 171
- . 1987, *A&A*, 186, 49
- Bressan, A., Chiosi, C., & Tantalo, R. 1996, *A&A*, 311, 425
- Bruzual A., G., & Charlot, S. 1993, *ApJ*, 405, 538
- Buzzoni, A. 1997, in *IAU Symp. 183, Cosmological Parameters and Evolution of the Universe*, ed. K. Sato (Dordrecht: Kluwer), 18
- Chandar, R., Bianchi, L., & Ford, H. C. 1999a, *ApJS*, 122, 431
- . 1999b, *ApJ*, 517, 668
- . 2001, *A&A*, 366, 498
- Chandar, R., Bianchi, L., Ford, H. C., & Salasnich, B. 1999c, *PASP*, 111, 794
- Charlot, S., & Bruzual A., G. 1991, *ApJ*, 367, 126
- Chiosi, C., Bressan, A., Portinari, L., & Tantalo, R. 1998, *A&A*, 339, 355
- Christian, C. A., & Schommer, R. A. 1982, *ApJS*, 49, 405
- . 1983, *ApJ*, 275, 92
- . 1988, *AJ*, 95, 704
- Ciani, A., D'Odorico, S., & Benvenuti, P. 1984, *A&A*, 137, 223
- Fan, X., et al. 1996, *AJ*, 112, 628
- Fioc, M., & Rocca-Volmerange, B. 1997, *A&A*, 326, 950
- Freedman, W. L., Wilson, C. D., & Madore, B. F. 1991, *ApJ*, 372, 455
- Galadí-Enríquez, D., Trullols, E., & Jordi, C. 2000, *A&AS*, 146, 169
- Hiltner, W. A. 1960, *ApJ*, 131, 163
- Jablonka, P., Bica, E., Pelat, D., & Alloin, D. 1996, *A&A*, 307, 385
- Kennicutt, R. C. 1998, *ARA&A*, 36, 189
- Kong, X., et al. 2000, *AJ*, 119, 2745
- Kron, G. E., & Mayall, N. U. 1960, *AJ*, 65, 581
- Landolt, A. U. 1983, *AJ*, 88, 439
- . 1992, *AJ*, 104, 340
- Leitherer, C., et al. 1996, *PASP*, 108, 996
- . 1999, *ApJS*, 123, 3
- Ma, J., Zhou, X., Chen, J., Wu, H., Jiang, Z., Xue, S., & Zhou, J. 2002, *A&A*, in press
- Ma, J., Zhou, X., Kong, X., Wu, H., Chen, J., Jiang, Z., Zhu, J., & Xue, S. 2001, *AJ*, 122, 1796
- Melnick, J., & D'Odorico, S. 1978, *A&AS*, 34, 249
- Mochejska, B. J., Kaluzny, J., Krockenberger, M., Sasselov, D. D., & Stanek, K. Z. 1998, *Acta Astron.*, 48, 455
- Schaerer, D., & de Koter, A. 1997, *A&A*, 322, 598
- Schaerer, D., & Vacca, W. D. 1998, *ApJ*, 497, 618
- Schmidt, A. A., Bica, E., & Alloin, D. 1990, *MNRAS*, 243, 620
- Searle, L., Sargent, W. L. W., & Bagnuolo, W. G. 1973, *ApJ*, 179, 427
- Stetson, P. B. 1987, *PASP*, 99, 191
- . 1992, in *ASP Conf. Ser. 25, Astronomical Data Analysis Software and Systems I*, ed. D. M. Worrall, C. Biemesderfer, & J. Barnes (San Francisco: ASP), 297
- Tinsley, B. M. 1972, *A&A*, 20, 383
- Yan, H. J., et al. 2000, *PASP*, 112, 691
- Zheng, Z. Y., et al. 1999, *AJ*, 117, 2757
- Zhou, X., Jiang, Z., Wu, H., Xue, S., Ma, J., Chen, J., Zhu, J., & Windhorst, R. 2001a, *A&AS*, submitted
- Zhou, X., Jiang, Z.-J., Xue, S.-J., Wu, H., Ma, J., & Chen, J.-S. 2001b, *Chinese Astron. Astrophys.*, 1, 372
- Zombeck, M. V. 1990, *Handbook of Space Astronomy and Astrophysics* (2d. ed; Cambridge: Cambridge Univ. Press)